Journal of Power Sources 185 (2008) 1315–1321

Contents lists available at ScienceDirect

Journal of Power Sources

journal homepage: www.elsevier.com/locate/jpowsour

FeCr gas diffusion layer with surface modification for fuel processing in direct-methane solid oxide fuel cells

Ta-Jen Huang*, Meng-Chin Huang

Department of Chemical Engineering, National Tsing Hua University, Hsinchu 300, Taiwan, ROC

ARTICLE INFO

Article history:
Received 8 September 2008
Accepted 10 September 2008
Available online 20 September 2008

Keywords:
Gas diffusion layer
Surface modification
Fuel processing
Methane
Solid oxide fuel cell
FeCr alloy

ABSTRACT

A solid oxide fuel cell (SOFC) with an Ni-YSZ anode was tested both without and with porous FeCr disk as a gas diffusion layer (GDL) under direct methane feeding. The surface of GDL was modified by coating with YSZ or Ni-YSZ powders. When gold mesh was used as the current collector, the performance of the direct-methane SOFC degraded very quickly. When FeCr GDL was used as the current collector over the anode, the performance became better and stable. Surface modification of GDL increased the current density. Both in GDL and over the anode, the major methane reaction was CH_4 dissociation, which yielded C species. The C species produced in GDL can be removed via gasification by carbon dioxide that forms over the anode. The formation of CO_2 can become the major reaction in the GDL of FeCr + YSZ while that of CO is the major reaction in the GDL of either FeCr or FeCr + Ni-YSZ. The electrochemical oxidation of CO formed in GDL increases the current density. The electrochemical promotion of lattice-oxygen extraction promotes the oxidation of CO and C species over the anode.

© 2008 Elsevier B.V. All rights reserved.

1. Introduction

Methane has become an important fuel for solid oxide fuel cells (SOFCs). Hence, considerable research effort has been made into the conversion of methane fuel into hydrogen-rich gas, as required by the electrochemical reaction on the anode. Recently, internal reforming SOFCs have attracted substantial attention since they can eliminate the requirement for a separate fuel reformer and also markedly reduce the need for cell cooling, which is usually performed by the flow of excess air through the cathode [1]. Depending on the operating conditions, the heat consumed by internal reforming can vary from 40 to 70% of the total heat produced in a fuel cell [2]. Therefore, internal reforming SOFC is an energy-efficient system design. However, carbon deposition over the usual Ni-cermet anode is a well-known problem when methane is used as fuel. Although the carbon deposition problem may be overcome by adding sufficient steam into the fuel stream, dilution of the fuel by the steam becomes a problem [2]; also, extra heating energy is required to generate the steam. Direct-methane SOFCs with either an inert porous layer [3] or a catalytic layer [4] placed between the anode and the fuel stream have potential to solve the problem of carbon deposition.

Methane decomposes over the Ni-cermet anodes in direct-methane SOFCs [5,6]. Methane decomposition over Ni is usually considered as proceeding as $CH_4 \rightarrow CH_3 + H \rightarrow CH_2 + H_2 \rightarrow CH + H + H_2 \rightarrow C + 2H_2$. At high temperatures, such as 800 °C, $CH_4 \rightarrow C + 2H_2$ may occur directly, as in the thermal cracking of methane. Thus, the decomposition of methane over Ni generally causes the deposition of carbon (coking) [7], potentially causing very rapid deactivation of the SOFC anode; consequently, the removal of the deposited carbon should be important. However, a carbon SOFC that utilizes the deposited carbon as a fuel has been proposed [8]. Huang and Huang [9] confirmed that the deposited carbon can be fully utilized for power generation. However, the deposited C species may lift the Ni species off the surface [10], such that the amount of deposited carbon should be controlled; the latter may be done using a low concentration of methane, a short feeding time of methane, or the continuous removal of the deposited C species.

The removal of the deposited carbon from methane decomposition can proceed via CO_2 de-coking [10], which involves gasification of the deposited carbon by carbon dioxide, which is a product of the anodic electrochemical reaction with methane as a fuel. Recently, Huang et al. [11–13] demonstrated that the deposited carbon can be gasified by the O species of the oxygen-ion conducting materials. In this case, the removal of the deposited carbon by carbon dioxide may proceed as $CO_2 \rightarrow CO + O$, and then the O species fills the oxygen vacancy of the oxygen-ion conducting materials to become a lattice oxygen [11,12]; then, the C species may react with the lattice oxygen to produce CO or CO_2 [14].

* Corresponding author. Tel.: +886 3 5716260; fax: +886 3 5715408.
E-mail address: tjhuang@che.nthu.edu.tw (T.-J. Huang).

0378-7753/$ – see front matter © 2008 Elsevier B.V. All rights reserved.
doi:10.1016/j.jpowsour.2008.09.040

FeCr alloy can be adopted as an interconnect material for intermediate temperature SOFCs [15]. Thus, FeCr can be utilized as the current collector over the SOFC anode. In this work, a porous FeCr disk with or without surface modification was used as the gas diffusion layer (GDL) and as the current collector to replace the anode-side gold mesh during direct-methane SOFC (DM-SOFC) tests. The surface was modified by adding yttria-stabilized zirconia (YSZ) and Ni-YSZ powders, of which the latter has the same composition as that of the anode. When a gold mesh was used as the current collector over the anode side, the performance of a direct-methane SOFC degraded very quickly; however, FeCr GDL without or with surface modification resulted in an improved and stabilized DM-SOFC performance.

2. Experimental

2.1. Preparation of porous FeCr disk

A porous FeCr disk was prepared by mixing FeCr powder (Goodfellow, Fe 87.5% and Cr 12.5%, particle size 45 μm) and graphite powder (Aldrich, synthetic, particle size <20 μm) in a weight ratio of graphite:FeCr of 3:4. 0.5 g of the mixture powder was compressed under 10 ton into a disk. Then, the disk was calcined at 1200 °C to make it porous. The disk had a porosity of 78%, an area of 1 cm^2, and a thickness of 0.22 cm.

The surface of the porous FeCr disk was modified by physically mixing 0.075 g of YSZ powder or Ni-YSZ powder with the disk; intensive shaking was performed in an effort to distribute the powders uniformly in the pores of the FeCr disk. Then, the disk was calcined at 800 °C to fix the powders to the FeCr surface.

2.2. Preparation of Ni-YSZ powder

The Ni-YSZ powder was prepared by impregnating the YSZ (8 mol% yttria) powder (1.68 μm) with an aqueous solution of nickel nitrate (98% purity) to make Ni 60 wt.% with respect to YSZ. The mixture was heated with stirring to remove excess water and then placed in a vacuum oven to dry overnight. The dried Ni-YSZ powder was heated to 900 °C and then cooled to room temperature. After milling, the Ni-YSZ powder was Ni:YSZ = 3:5 by weight, i.e., 60 wt.% Ni-YSZ.

2.3. Construction of the SOFC unit

The commercial YSZ tape (156 μm thickness, Jiuhow, Taiwan) was employed to make an electrolyte-supported cell. A disk with a diameter of 1.25 cm was cut from the tape. One side of the disk was coated with the Ni-YSZ paste, which was made of the above Ni-YSZ powder, corn oil, polyvinyl butyral and ethanol. The other side of the disk was screen-printed with a thin layer of Pt paste (Heraeus, C3605P) to make the cathode layer.

The method by which the Ni-YSZ paste was coated on the YSZ disk to make the anode layer has been described elsewhere [9]. The thus-prepared unit cell has an anode area of 1 cm^2, an anode thickness of about 30 μm, an electrolyte thickness of 156 μm, a cathode area of 1 cm^2 and a cathode thickness of about 5 μm. These thicknesses were measured from a scanning electron micrograph plot of the cross section of the unit cell.

Both sides of the completed unit cell were connected, respectively, to gold mesh wires (100 mesh), or to the FeCr disk on the anode side, to collect the current, and then using Pt wires to the current and voltage measurement units. The ceramic paste was used to seal the unit cell in a quartz tube with heat treatment at 400 °C for 1.5 h to complete the preparation of the test unit. The anode side of the unit cell was sealed in a quartz tube and the cathode side was exposed to stagnant air.

2.4. Activity tests of unit cell

A voltage of 0.61 V was maintained during all tests in this work. The test temperature was fixed at 800 °C. The fuel to the anode side was 10.5% methane (CH_4) in argon; for reduction, the feed to the anode side was 10% H_2 in argon. The flow rate past the anode side was always 100 ml min^{-1}.

The test started with the reduction of the anode at 400 °C in 10% H_2 for 1 h. Then, a pure argon flow was used to purge the system for 2 h. The test unit was then heated in argon to 800 °C at a rate of 5 °C min^{-1}. Then, 10% H_2 was introduced for 30 min and argon flow continued until the measured electrical current became zero. A direct-methane SOFC test was then performed with the introduction of 10.5% CH_4 flow for 360 min. Then, the anode-side flow was switched to argon.

During the test, electrical current, voltage and outlet gas compositions were continuously measured. The CO and CO_2 contents were measured by CO-NDIR and CO_2-NDIR (non-dispersive infrared analyzer, Beckman 880), respectively. Other gas compositions were measured using two gas chromatographs (China Chromatography 8900) in series.

3. Results

3.1. Effect of FeCr gas diffusion layer on DM-SOFC performance

Fig. 1 shows the results of a direct-methane SOFC without a gas diffusion layer—that is, with gold mesh as the current collector over the anode side. The methane conversion rate decreases continuously with the operation time, as shown in Fig. 1(a). Fig. 1(a) also shows that, before about 150 min, the methane conversion rate exceeded the ($CO + CO_2$) formation rate, indicating the deposition of carbon species over the anode. The formation of the deposited C species is revealed by the carbon balance:

$$\Delta CH_4 - \Delta(CO + CO_2) = \Delta C \quad (1)$$

where ΔCH_4 is the methane conversion rate, $\Delta(CO + CO_2)$ is the rate of formation of CO plus CO_2, and ΔC is the rate of formation of the deposited C species.

Fig. 1(a) also shows that, except during the first 10 min of SOFC operation, no H_2O is formed, indicating that the major reaction of CH_4 during DM-SOFC operation is the dissociation of methane:

$$CH_4 \rightarrow C + 2H_2 \quad (2)$$

The hydrogen balance is thus $\Delta H_2 = 2\Delta CH_4$, as confirmed by the results that is also shown in Fig. 1(a). If the C species is not oxidized to form CO and/or CO_2, it becomes the deposited carbon species. The deposited carbon species cover the anode surface, degrading SOFC performance. Additionally, the covering of the anode by the C species causes hydrogen not to be adsorbed and thus not to be oxidized to form H_2O, as shown by the results without H_2O formation; thus, the hydrogen that was produced in reaction (2) was not consumed, yielding $\Delta H_2 = 2\Delta CH_4$ as shown in Table 1. This indicates that the interaction of the C species with the catalyst surface is stronger than that of hydrogen; restated, hydrogen cannot compete with the C species to be adsorbed onto the anode Ni surface. However, the rate of CO formation decreases appreciably but the CO_2 formation rate decreases only slightly, as shown in Fig. 1(b).

Fig. 2 shows that the current density of DM-SOFC without GDL decreases continuously as the SOFC operation proceeds. Adding an FeCr GDL, which acts also as a current collector, causes the current density to increase continuously, as also shown in Fig. 2. A

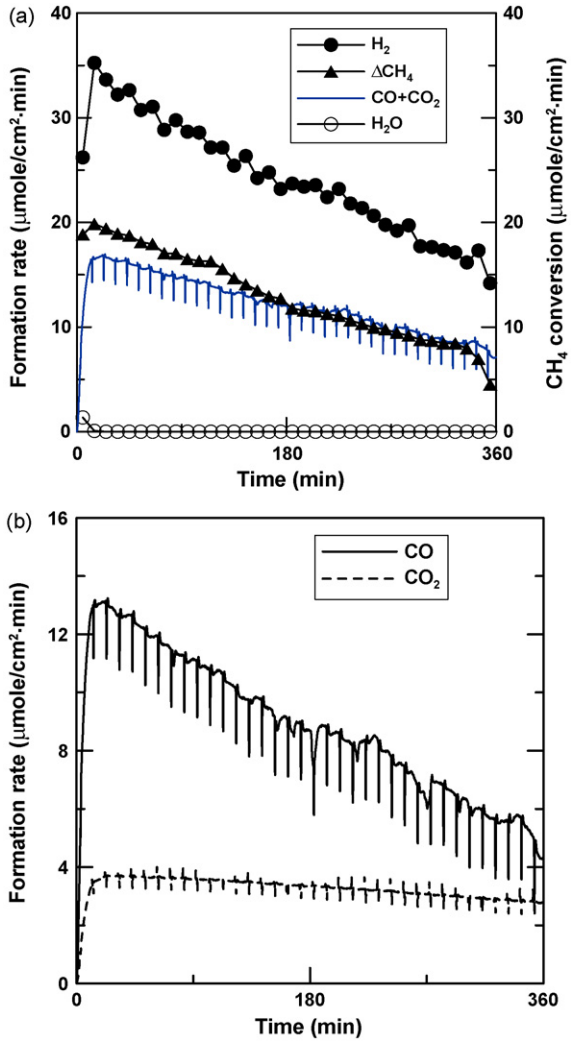

Fig. 1. Without the gas diffusion layer. (a) H_2, $CO+CO_2$, H_2O formation rates and CH_4 conversion rate and (b) CO and CO_2 formation rates.

comparison of Fig. 3(a) with Fig. 1(a) shows that, adding the FeCr GDL appreciably changes the behavior of the rates of formation of the products, indicating that fuel processing should have occurred in GDL. Section 4 will clarify reactions for processing fuel in GDL.

3.2. Effect of surface modification

Fig. 2 also shows that modifying the surface of the FeCr GDL with YSZ powder, forming FeCr + YSZ, increases the current density. Modifying the surface of the FeCr GDL with Ni-YSZ powder, forming FeCr + Ni-YSZ, further increases the current density.

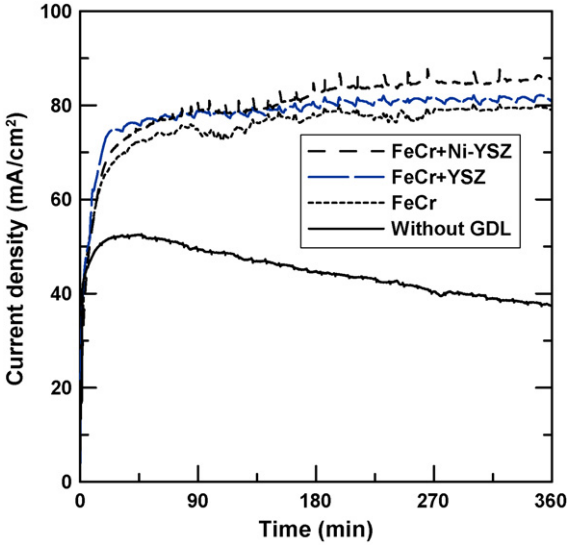

Fig. 2. A comparison of the measured currents without GDL and with GDL plus surface modification.

Fig. 3 shows that modifying the surface of the FeCr GDL changes the behavior of the rates of product formation—especially when the surface is modified by the oxygen-ion conducting materials of YSZ. No H_2O is formed from the very beginning of the SOFC operation. Additionally, ΔH_2 equals $2\Delta CH_4$ exactly in the steady state, as shown in Table 1, indicating that the major CH_4 reaction during DM-SOFC operation, both in GDL and over the anode, is the methane dissociation reaction (2). Section 4 will clarify the fuel-processing reactions in GDL without or with surface modification and the associated electrochemical reactions over the anode.

3.3. Electrochemical behavior

Comparing Fig. 3 with Fig. 2 reveals that the behavior of $(CO+CO_2)$ formation, which consumes the oxygen species that presumably come from the cathode, differs substantially from that of current density, which is generated by oxygen ions from the cathode. Fig. 4 thus presents the profiles of overall measured and equivalent currents to clarify this behavior. Notably, the equivalent current is the current that would be produced were the O species for the formation of the oxidation products at the anode to have come from the cathode. In this work, the detectable oxidation products were CO, CO_2 and H_2O. However, in the cases shown in Fig. 4, the equivalent current is equivalent only to the formation rate of $(CO+CO_2)$, because the H_2O formation rate is zero during the entire operation period, as shown in Fig. 3. Thus, the equivalent current is calculated as [(CO formation rate) + (CO_2 formation rate) × 2]/0.31088. Notably, also, a current density of 1 mA cm^{-2} is equivalent to an oxygen transfer rate of 0.31088 μmol O^{2-} cm^{-2} min^{-1}.

Table 1
Steady-state[a] current density, methane conversion and product formation rates, and CO_2 selectivity.

SOFC unit with GDL of	Current density (mA cm^{-2})	ΔCH_4[b]	H_2[c]	CO_2[c]	CO[c]	CO_2 selectivity[d]
FeCr	78.20	22.0	44.0	7.61	12.39	0.380
FeCr + YSZ	81.01	22.0	44.0	9.76	11.77	0.453
FeCr + Ni-YSZ	84.54	23.8	47.6	8.25	14.22	0.367

[a] Designated by the SOFC operation period from 200 to 300 min. The reported value is the averaged value.
[b] Methane conversion rate in μmol cm^{-2} min^{-1}.
[c] Formation rate in μmol cm^{-2} min^{-1}.
[d] Defined as $CO_2/(CO+CO_2)$.

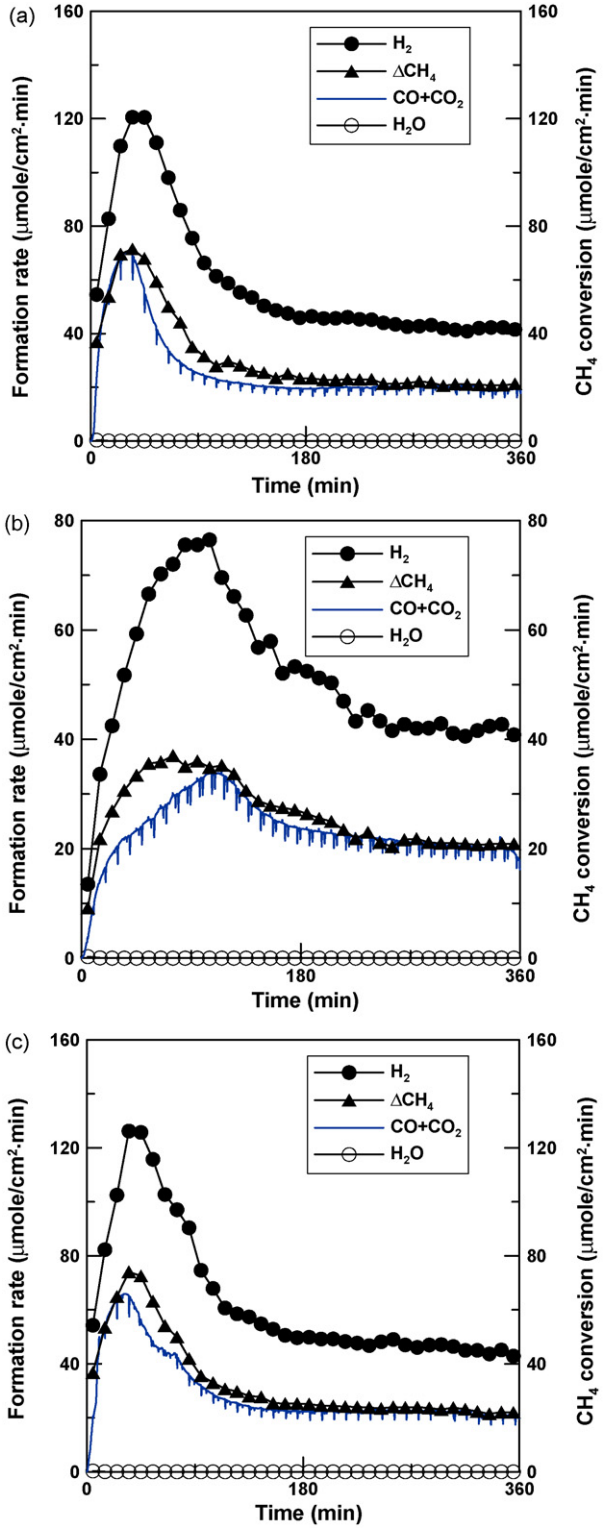

Fig. 3. H_2, $CO + CO_2$, H_2O formation rates and CH_4 conversion rate in SOFC unit with the GDL of (a) FeCr; (b) FeCr + YSZ; and (c) FeCr + Ni-YSZ.

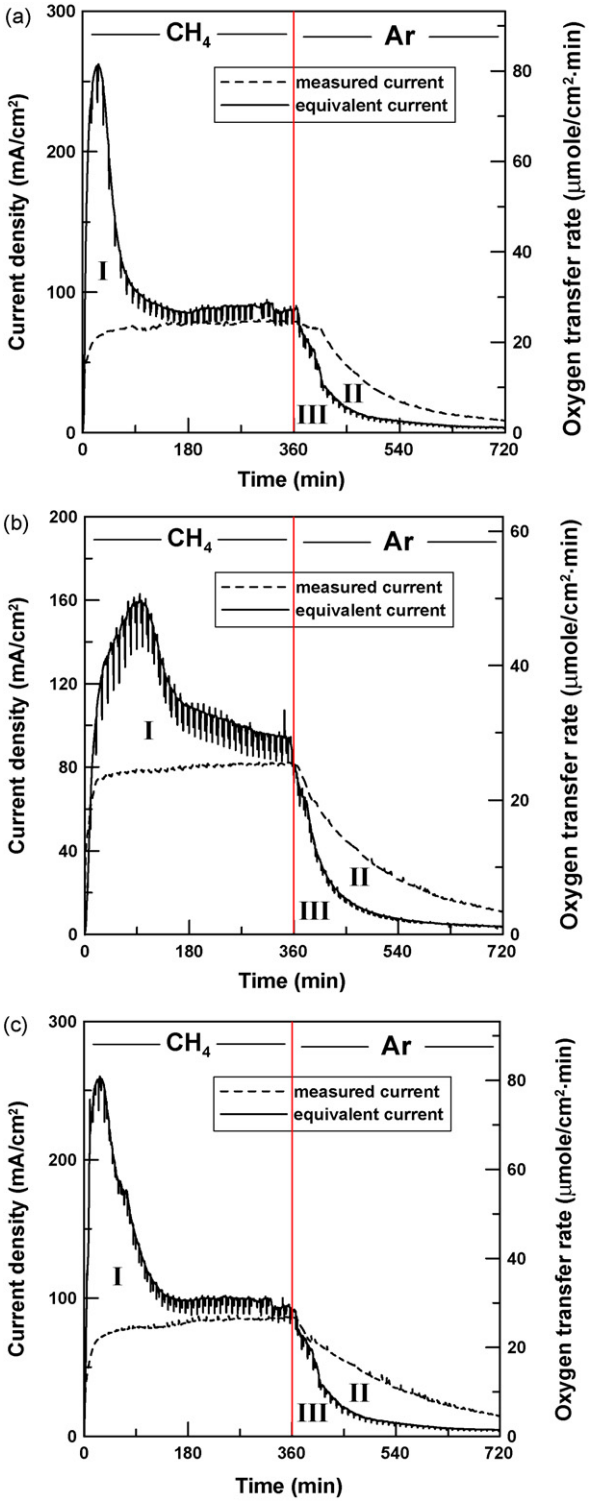

Fig. 4. Overall measured and equivalent currents in SOFC unit with the GDL of (a) FeCr; (b) FeCr + YSZ; and (c) FeCr + Ni-YSZ. Zone I denotes the area between the curves of equivalent current and measured current and extends from time zero until the meeting of these two curves; zone II denotes the area under the curve of measured current to the right of the curve of equivalent current; zone III denotes the area under the curve of equivalent current during Ar flow.

Fig. 4 shows the formation of zones I, II and III. Notably, zone I denotes the area between the curves of the equivalent current and the measured current, and extends from time zero until the meeting of these two curves; zone II denotes the area under the curve of the measured current to the right of the curve of the equivalent current, and zone III denotes the area under the curve of equivalent current during Ar flow.

According to Huang and Huang [9,16–18], in an SOFC unit without GDL, in zone I, lattice-oxygen extraction is electrochemically promoted to oxidize the carbon species and in zone II, the extracted lattice oxygen is replenished by the oxygen species from the cathode via the electrolyte; this oxygen replenishment results in a fuel-free current [9]. Additionally, zone III arises from the removal of the deposited carbon species via gasification by oxidation [18]. However, in DM-SOFCs with GDL as the current collector, the electrochemical promotion of lattice-oxygen extraction for the oxidation of the carbon species may occur at both the anode and the GDL. Therefore, the materials for modifying the surface of GDL can change the reaction behavior, as indicated by the variation in zone I behavior with surface modification, as shown in Fig. 4. Section 4 will clarify the effect of these differences in association with the reactions over the anode and in GDL.

3.4. CO and CO_2 formation rates

For methane reactions in direct-methane SOFCs, the formation of only CO and not CO_2 should result in a large variation in the fuel efficiency for power generation, because the electrochemical formation of CO_2 involves four electrons, while that of CO involves only two electrons, with each oxygen ion's carrying two electrons; thus, the current density associated with the formation of CO_2 is two times that associated with the formation of CO as measured by the utilization of carbon in methane. Fig. 5 presents the rates of formation of CO and CO_2 in DM-SOFCs with FeCr GDL without and with surface modification. The rate of CO_2 formation changes considerably, especially upon surface modification by oxygen-ion conducting materials of YSZ.

Fig. 5(b) shows that, in the operation of the SOFC unit with a GDL of FeCr + YSZ, there is mainly CO_2 formation in the first 90 min, with no CO formation or with the formation of much less CO. However, in the SOFC unit with GDL of either FeCr or FeCr + Ni-YSZ, mainly CO is formed in the first 90 min of operation. This difference between the formations of CO_2 and CO is determined by the presence of YSZ, which has an oxygen storage capacity because its bulk oxygen vacancies, which contain lattice oxygen. Section 4 will explain this fact in association with the major reactions in GDL and over the anode.

4. Discussion

4.1. Reactions in GDL and over the anode

According to the above results, the major reaction of methane is its dissociation (2), which occurs not only over the anode but also in GDL, as presented in Fig. 6. Notably, the proposed reaction schemes show only how a stable SOFC performance may be achieved; since many interconnecting reactions are involved, complete reaction schemes demand further study.

Figs. 3–5 show that the behavior of SOFC with the GDL of FeCr + Ni-YSZ is similar to that with the GDL of FeCr but different from that with the GDL of FeCr + YSZ, respectively, because Ni-YSZ consists of 60 wt.% Ni, which should cover most of the YSZ surface; thus, the function of the lattice oxygen of YSZ in Ni-YSZ powder should be much lower than that of pure YSZ powder for the GDL

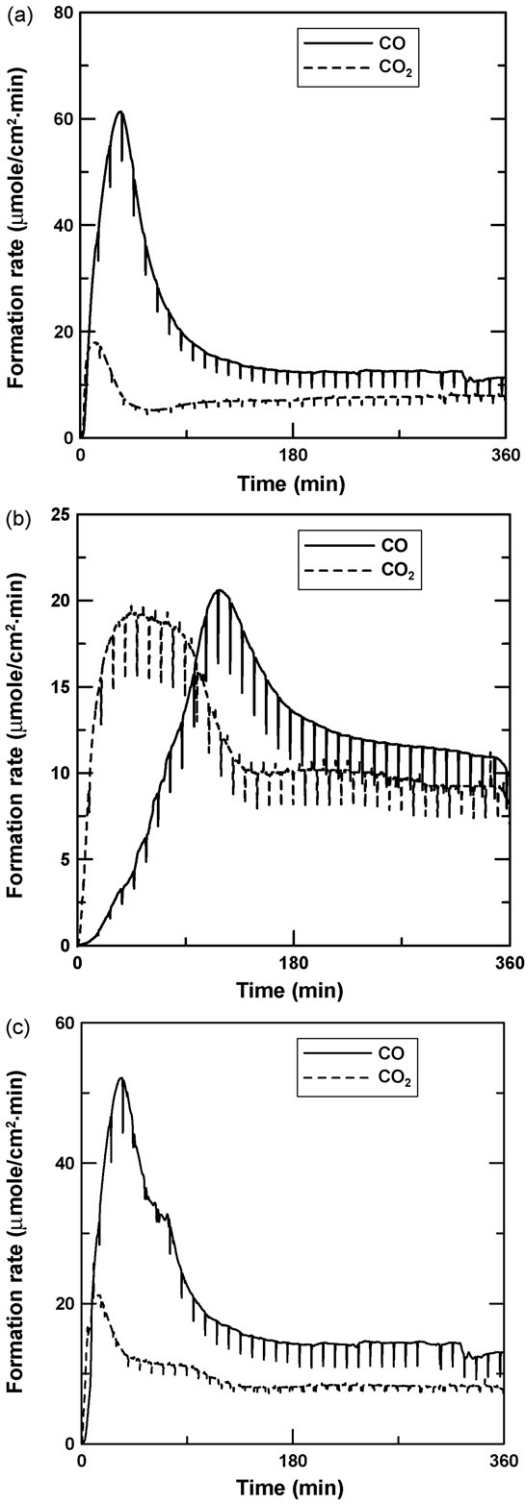

Fig. 5. CO and CO_2 formation rates in SOFC unit with the GDL of (a) FeCr; (b) FeCr + YSZ; and (c) FeCr + Ni-YSZ.

of FeCr + YSZ, such that either FeCr or FeCr + Ni-YSZ can be considered to consist mainly of metal surface. Therefore, the type of GDL can be classified, according to SOFC behavior, as either GDL with a metal surface or GDL with a YSZ surface. Notably, the higher activity of FeCr + Ni-YSZ than that of FeCr, as shown in Table 1, is related to the higher methane activity of Ni than that of Fe [14]. Notably, also, under reducing conditions at 800 °C, some iron oxide may be

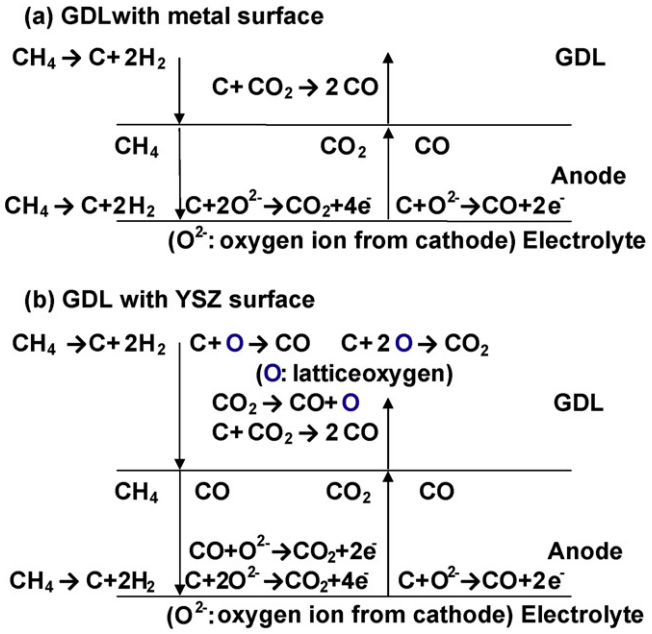

Fig. 6. Schemes of the major reactions in GDL and over the anode of direct-methane SOFCs during steady state. (a) GDL with metal surface; (b) GDL with YSZ surface.

reduced to Fe metal [14] and all nickel oxide can be reduced to Ni metal [10]; the fact that an FeCr porous layer was used as a current collector in this work means that an appreciable amount of iron oxide must have been reduced to iron metal.

Over the anode, the C species produced by methane dissociation can react electrochemically with the oxygen-ion species (O^{2-}) from the cathode to produce CO_2 and CO [18]:

$$C + 2O^{2-} \rightarrow CO_2 + 4e^- \quad (3)$$

$$C + O^{2-} \rightarrow CO + 2e^- \quad (4)$$

Notably, CO_2 is preferred to increase fuel efficiency, since the formation of more CO_2 results in a higher current density. When CO_2 is carried from the anode to GDL, the C species produced in GDL can be removed via gasification by carbon dioxide [10]:

$$C + CO_2 \leftrightarrows 2CO \quad (5)$$

Notably, reaction (5) is backward CO disproportionation.

Over GDL with a metal surface, the methane dissociation reaction (2) and the associated de-coking reaction (5) dominate, as presented in Fig. 6(a). Notably, in a direct-methane SOFC without GDL, as in Fig. 6(a) except for the lack of GDL, there is no de-coking reaction (5); additionally, the extent of methane dissociation over the anode should exceed that with GDL, where methane dissociation consumes a substantial amount of methane, so that the amount of methane that reaches the anode is reduced considerably. Therefore, a direct-methane SOFC without GDL deactivates while that with FeCr GDL performs stably, as shown in Fig. 2.

However, the C species produced in GDL can be removed by the lattice oxygen of the GDL materials by the following reaction [19]:

$$C + O \leftrightarrows CO \quad (6)$$

$$C + 2O \leftrightarrows CO_2 \quad (7)$$

Notably, the consumption of the lattice oxygen generates the oxygen vacancy, which can be replenished by the O species that are produced by the reaction [12],

$$CO_2 \leftrightarrows CO + O \quad (8)$$

Therefore, the cathode-side O species can be carried over to GDL in the form of CO_2; that is, the cathode-side O species is transported to the anode in the form of O^{2-}, which oxidizes the C species to form CO_2 by reaction (3) and then CO_2 is carried over to GDL to be consumed in reaction (8) producing O species that fill the oxygen vacancies, as shown in Fig. 6(b). Thus, the pathway of O replenishment is from the cathode-side gas-phase oxygen to the anode and then to GDL; that is, the formation of CO_2 over the anode consumes the O species from the cathode, in the form of oxygen ions, and CO_2 is then transported from the anode to GDL as a source of O species.

CO formed in GDL can be carried over to the anode and the following reaction can occur;

$$CO + O^{2-} \rightarrow CO_2 + 2e^- \quad (9)$$

Fig. 6(b) presents these major reactions (2)–(9) to clarify the relationship between the reactions in GDL and those over the anode.

The occurrence of reaction (9) is key to the enhancement of current density. Table 1 shows that, with exactly the same CH_4 conversion, the SOFC unit with the GDL of FeCr + YSZ has a higher current density than that of FeCr, because the lattice oxygen of YSZ, which enhances the rate of the formation of CO, according to reaction (6); this enhanced rate of CO formation results in an enhanced current density, according to reaction (9). Notably, with the same rate of CH_4 conversion but without reaction (9), the current density in the SOFC unit with GDL of FeCr + YSZ cannot be distinguished from that of FeCr since both SOFC units have the same anode; that is, the electrochemical activity of the anode should be the same and thus the current density would be the same for the same CH_4 conversion.

In GDL and over the anode, other reactions may also occur. Notably, the CO_2 reforming of methane occurs in GDL with surface modification by YSZ, which contains oxygen vacancy and lattice oxygen. Notably, the CO_2 reforming of methane consists of the dissociation of methane and CO_2 as well as the gasification of the surface carbon species by lattice oxygen [20], which are reactions (2) and (6)–(8). These reactions occur in GDL with YSZ surface, as shown in Fig. 6(b); thus, the CO_2 reforming of methane can occur in GDL.

4.2. Behavior of CO and CO_2 formation

For the SOFC unit with a GDL of FeCr + YSZ, the behavior of the formation of mainly CO_2 during the period when mainly CO is formed in FeCr or FeCr + Ni-YSZ, both having mainly metal surface, is also considered to be due to the lattice oxygen of YSZ. However, the metal surface can be oxidized and lattice oxygen can exist for the oxidation of the deposited C species, so reactions (6) and (7) can occur; nevertheless, the extent of reactions (6) and (7) should be much less than those over the surface of YSZ, which has a high oxygen storage capacity; thus, reactions (6) and (7) are not the major reactions in GDL with a metal surface and are not presented in Fig. 6(a). Therefore, the formation of CO_2 becomes the major reaction in FeCr + YSZ while the formation of CO is the major reaction in both FeCr and FeCr + Ni-YSZ, as shown in Fig. 5.

Although reaction (8) can oxidize the metal to store some oxygen species in both FeCr and FeCr + Ni-YSZ, the oxygen storage capacity of YSZ increases the concentration of oxygen species in FeCr + YSZ, promoting the formation of CO_2. Thus, CO_2 selectivity can increase. Table 1 shows that, in the steady state, CO_2 selectivity associated with FeCr + YSZ exceeds that associated with either FeCr or FeCr + Ni-YSZ. In FeCr + Ni-YSZ, the YSZ surface is covered by the high Ni loading such that its YSZ function is limited; the high loading of Ni results in a high rate of methane conversion, as also

Table 2
Total amount of oxygen extracted from the anode side during 360 min of CH_4 flow.

SOFC unit with GDL of	Oxygen extracted from the anode side[a] ($\times 10^3$ μmol cm^{-2} min^{-1})
FeCr	3.79
FeCr + YSZ	3.83
FeCr + Ni-YSZ	5.02

[a] Calculated from the total area of zone I.

shown in Table 1, leading to a large amount of carbon deposition, reducing CO_2 selectivity due to limited oxygen supply.

4.3. Electrochemical promotion of lattice-oxygen extraction

The variation in zone I behavior with surface modification, as shown in Fig. 4 can also be explained by the oxygen storage capacity of YSZ. As described above, the formation of CO_2 is enhanced by the oxygen storage capacity of YSZ. Thus, less CO is carried to the anode to be oxidized electrochemically by the oxygen ion via reaction (9). However, CO can also be oxidized by extracting the lattice-oxygen species of the anode-side electrolyte materials; this lattice-oxygen extraction is due to the effect of electrochemical promotion [9,16–18]. Less CO over the anode may result in less lattice-oxygen extraction. Therefore, the SOFC unit with a GDL of FeCr-YSZ exhibits less lattice-oxygen extraction than either FeCr or FeCr + Ni-YSZ in the first 60 min of operation, as shown in Fig. 4.

Since the total amount of electrochemically promoted lattice-oxygen extraction is limited [18,21], the SOFC unit with a GDL of FeCr-YSZ is associated with more lattice-oxygen extraction than either FeCr or FeCr + Ni-YSZ after about 60 min of operation, as also shown in Fig. 4. Additionally, Table 2 shows that the total amount of lattice-oxygen extraction increases in the order FeCr < FeCr + YSZ < FeCr + Ni-YSZ, in accordance with increasing current density as shown in Table 1. However, the amount of extracted lattice oxygen in the SOFC unit with a GDL of FeCr + Ni-YSZ largely exceeds that in the SOFC unit with a GDL of FeCr + YSZ, perhaps because of the electrochemically promoted lattice-oxygen extraction in GDL; notably, the Ni-YSZ powder in the GDL of FeCr + Ni-YSZ is the same as that of the anode; however, this claim must be clarified by further study.

After the lattice oxygen is extracted from the anode-side electrolyte materials, a deficiency of the lattice-oxygen concentration induces the replenishment of the lattice oxygen from the cathode side. Notably, the lattice-oxygen replenishment generates an electrical current [16–18]. The small jumping or oscillatory behavior of the current density, shown in Fig. 2, may be due to a variation in the lattice-oxygen replenishment rate in association with the variation in the lattice-oxygen concentration deficiency. Since the lattice-oxygen concentration affects CO and CO_2 formation rates, its variation may be associated with the oscillatory behavior of CO and CO_2 formation rates, as shown in Figs. 1(b) and 5. However, this possibility also requires further study.

5. Conclusions

1. When gold mesh was used as the current collector, the performance of the direct-methane SOFC degraded very quickly. When the FeCr GDL with or without surface modification was used as the current collector over the anode, the performance became better and stable.
2. Modifying the surface of the FeCr GDL with either YSZ or Ni-YSZ powders increased the current density.
3. Both in GDL and over the anode during direct-methane SOFC operation, the major methane reaction was CH_4 dissociation to produce the C species, which can be oxidized by the lattice oxygen to form CO.
4. The electrochemical oxidation of CO that was formed in the GDL and carried to the anode increases the current density.
5. The C species produced in GDL can be removed via gasification by carbon dioxide that forms over the anode.
6. The formation of CO_2 can become the major reaction in the GDL of FeCr + YSZ while that of CO is the major reaction in the GDL of either FeCr or FeCr + Ni-YSZ.
7. The electrochemical promotion of lattice-oxygen extraction promotes the oxidation of CO and C species over the anode.

References

[1] P. Aguiar, D. Chadwick, L. Kershenbaum, Chem. Eng. Sci. 57 (2002) 1665.
[2] P. Aguiar, C.S. Adjiman, N.P. Brandon, J. Power Sources 138 (2004) 120.
[3] Y. Lin, Z. Zhan, S.A. Barnett, J. Power Sources 158 (2006) 1313.
[4] Y. Yin, S. Li, C. Xia, G. Meng, J. Power Sources 167 (2007) 90.
[5] J.B. Wang, J.C. Jang, T.J. Huang, J. Power Sources 122 (2003) 122.
[6] Y. Lin, Z. Zhan, J. Liu, S.A. Barnett, Solid State Ionics 176 (2005) 1827.
[7] C. Mallon, K. Kendall, J. Power Sources 145 (2005) 154.
[8] M. Ihara, K. Matsuda, H. Sato, C. Yokoyama, Solid State Ionics 175 (2004) 51.
[9] T.J. Huang, M.C. Huang, J. Power Sources 168 (2007) 229.
[10] J.B. Wang, Y.S. Wu, T.J. Huang, Appl. Catal. A: Gen. 272 (2004) 289.
[11] T.J. Huang, T.C. Yu, Catal. Lett. 102 (2005) 175.
[12] T.J. Huang, H.C. Lin, T.C. Yu, Catal. Lett. 105 (2005) 239.
[13] T.J. Huang, C.H. Wang, Chem. Eng. J. 132 (2007) 97.
[14] T.J. Huang, C.H. Wang, J. Power Sources 163 (2006) 309.
[15] W.Z. Zhu, S.C. Deevi, Mater. Sci. Eng. A348 (2003) 227.
[16] T.J. Huang, M.C. Huang, Chem. Eng. J. 135 (2008) 216.
[17] T.J. Huang, M.C. Huang, J. Power Sources 175 (2008) 473.
[18] T.J. Huang, M.C. Huang, Chem. Eng. J. 138 (2008) 538.
[19] T.J. Huang, C.H. Wang, Catal. Lett. 118 (2007) 103.
[20] J.B. Wang, S.Z. Hsiao, T.J. Huang, Appl. Catal. A: Gen. 246 (2003) 197.
[21] T.J. Huang, M.C. Huang, Int. J. Hydrogen Energy 33 (2008) 5073.